

Supplementary Information

Titanium(III) Member of the Family of Trigonal Building Blocks with Scorpionate and Cyanide Ligands

Andrew Brown,^a Mohamed Saber,^{a,b} Willem Van den Heuvel,^c Kelsey Schulte,^a Alessandro Soncini^c and Kim R. Dunbar*^a

^{a.} Department of Chemistry, Texas A&M University, College Station, TX 77843, USA

Fax: (+) 1 (979) 845-7177, E-mail: dunbar@chem.tamu.edu

^{b.} Current Address: Department of Chemistry, Fayoum University, Fayoum 63514, Egypt.

^{c.} School of Chemistry, University of Melbourne, Parkville, Victoria 3010, Australia

Experimental section

Starting Materials

The reagents $\text{TiCl}_3(\text{THF})_3$ (97%, Sigma-Aldrich), KTp^* (98%, TCI Chemicals), $[(\text{CH}_3\text{CH}_2)_4\text{N}]\text{Cl}$ (>98%, Sigma-Aldrich), anhydrous solvents diethyl ether (HPLC >99.9% inhibitor free, Sigma-Aldrich), and dimethylformamide (99.8%, Sigma-Aldrich) were purchased and used as received. Acetonitrile and tetrahydrofuran (ACS grade) were pre-dried over 3 Å molecular sieves and distilled under a dinitrogen atmosphere. The compound, $[(\text{CH}_3\text{CH}_2)_4\text{N}]\text{CN}$, was prepared by metathesis of $[(\text{CH}_3\text{CH}_2)_4\text{N}]\text{Cl}$ with NaCN in methanol followed by an extraction into CH_3CN , concentration, and precipitation with THF. Before using $[(\text{CH}_3\text{CH}_2)_4\text{N}]\text{CN}$ it was dried for 24 hours at ambient temperature in a distillation apparatus containing P_2O_5 . All reactions were conducted using standard Schlenk-line techniques or inside a nitrogen filled glovebox.

Preparation of $[(\text{CH}_3\text{CH}_2)_4\text{N}][\text{Tp}^*\text{TiCl}_3]$ (1). In a nitrogen purged glovebox, 5.0 g of $\text{TiCl}_3(\text{THF})_3$, 4.45g KTp^* , and 2.2g of $[(\text{CH}_3\text{CH}_2)_4\text{N}]\text{Cl}$ were added to a 200 mL Schlenk flask and charged with 100 mL CH_3CN . The dark purplish blue mixture was stirred for 24 hours and then filtered through a 30 mL glass fritted medium porosity frit to remove KCl . The filtrate was concentrated to ~30 mL which led to precipitation of the first crop of blue product. The remaining filtrate was concentrated to dryness, redissolved in a minimal volume of acetonitrile, filtered through a 30 mL medium porosity frit and treated with 150 mL of diethyl ether to produce a second crop of blue solid. At this stage, the filtrate was pinkish purple in color and

slow evaporation led to crystals of the by-product $[\text{Tp}^*\text{TiCl}_2\text{pz}^*]\text{pz}^*$ ($\text{pz}^* = 3,5$ -dimethylpyrazole), **2**. Adding a stoichiometric amount of $[(\text{CH}_3\text{CH}_2)_4\text{N}]\text{Cl}$ to an acetonitrile solution of $[\text{Tp}^*\text{TiCl}_2\text{pz}^*]\text{pz}^*$ led to the isolation of a third crop of blue solid which was collected on a 30 mL medium porosity frit. All three crops of solid were combined and redissolved in a minimal volume of acetonitrile. The blue solution was filtered and the filtrate was stored at $-15\text{ }^\circ\text{C}$ for 24 hours to give a crystalline product in a final yield of 6.3 g (80% based on $\text{TiCl}_3(\text{THF})_3$). IR (Nujol), $\nu(\text{BH})$, cm^{-1} : 2513; $\nu(\text{CH})$, cm^{-1} : 3129. Large block-shaped crystals of $[(\text{CH}_3\text{CH}_2)_4\text{N}][\text{Tp}^*\text{TiCl}_3]$ were grown by slow diffusion of diethyl ether into an acetonitrile solution of $[(\text{CH}_3\text{CH}_2)_4\text{N}][\text{Tp}^*\text{TiCl}_3]$ in a Schlenk tube after 1 week.

Preparation of $[(\text{CH}_3\text{CH}_2)_4\text{N}][\text{Tp}^*\text{Ti}(\text{CN})_3]$ (3**).** In the most successful experiment, 0.51 g $[(\text{CH}_3\text{CH}_2)_4\text{N}]\text{CN}$ were dissolved in 20 mL of CH_3CN and added slowly via pipette transfer to a stirring solution of 0.63g $[(\text{CH}_3\text{CH}_2)_4\text{N}][\text{Tp}^*\text{TiCl}_3]$ dissolved in 25 mL of CH_3CN . The resulting reaction mixture was stirred for 15 hours during which time a color transformation occurred from blue to green to brown and finally to orange. The reaction mixture was filtered through a 30 mL medium porosity glass frit to remove a dark blue impurity. The bright orange filtrate was concentrated to ~ 10 mL and treated with 90 mL of diethyl ether. The bright orange crude precipitate was collected by filtration: yield 0.55 g (92% based on $[(\text{CH}_3\text{CH}_2)_4\text{N}][\text{Tp}^*\text{TiCl}_3]$). IR (Nujol), $\nu(\text{CN})$, cm^{-1} : 2116, 2103; $\nu(\text{BH})$, cm^{-1} : 2521; $\nu(\text{CH})$, cm^{-1} : 3110. Crystals of $[(\text{CH}_3\text{CH}_2)_4\text{N}][\text{Tp}^*\text{Ti}(\text{CN})_3]$ were obtained from a 5mM solution of the crude powder containing 30% by volume acetonitrile in diethyl ether. Elemental analysis: Calcd. for **3** ($\text{C}_{26}\text{H}_{42}\text{B}_1\text{N}_{10}\text{Ti}_1$): C, 56.54; H, 7.48; N, 25.36. Found: C, 55.43; H, 7.44; N, 23.39; Cl, 0.00 %.

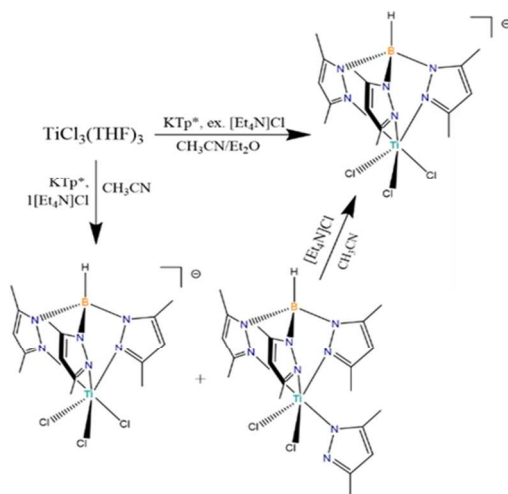


Chart S1. Synthetic routes to titanium starting materials.

Physical Methods

Infrared (IR) spectra were measured as Nujol mulls placed between KBr plates on a Nicolet 740 FT-IR spectrometer. Elemental analyses were performed by Atlantic Microlab, Inc. Thermogravimetric analysis was performed on a Shimadzu TGA-50 Analyzer. AC and DC magnetic susceptibility and magnetization measurements were collected using a Quantum Design MPMS-XL SQUID magnetometer. Dc magnetic susceptibility measurements were performed at an applied field of 1000 Oe over the temperature range 2-300 K. Dc magnetization data were collected at 1.8 K under a range of dc fields from 0-7 T. AC magnetic susceptibility measurements were performed in a 3 Oe ac measuring field at operating frequencies of 1-1500 Hz. The data were corrected for diamagnetic contributions as calculated from Pascal constants.¹ Single-crystal X-ray crystallographic data were collected on Bruker APEX diffractometers equipped with CCD detectors. The data sets were recorded as ω -scans at a 0.3° step width. Integration was performed with the Bruker SAINT² software package and absorption corrections were empirically applied using SADABS.³ The crystal structures were refined using the SHELX⁴ suite of programs.⁵ Images of the crystal structure were rendered using the crystal structure visualization software DIAMOND.⁶ All of the structures were solved by direct methods. Any remaining non-hydrogen atoms were located by alternating cycles of least squares refinements and difference Fourier maps. All hydrogen atoms were placed at calculated positions. The bond lengths of disordered solvent molecules were restrained to chemically meaningful values. Anisotropic thermal parameters were added for all non-hydrogen atoms.

X-ray Crystallography

Table S1. Crystal and structural refinement data for **1-3**.

	1	2	3
Empirical formula	C ₂₃ H ₄₂ BN ₇ TiCl ₃	C _{22.5} H _{33.5} BN ₉ TiCl ₂	C ₂₆ H ₄₂ BN ₁₀ Ti
Formula weight	581.69	559.17	553.40
Temperature/K	110.0	110.0	110.0
Crystal system	monoclinic	monoclinic	orthorhombic
Space group	Cc	C2/c	Pmn2 ₁
a/Å	17.669(4)	20.462(4)	11.634(2)
b/Å	10.410(2)	10.763(2)	8.1814(16)
c/Å	17.024(3)	25.135(5)	15.620(3)
α/°	90	90	90
β/°	111.44(3)	97.57(3)	90
γ/°	90	90	90
Volume/Å ³	2914.6(12)	5488(2)	1486.8(5)
Z	4	8	2
ρ _{calc} /cm ³	1.326	1.3536	1.236
F(000)	1228.0	2341.3	590.0
Radiation	MoKα (λ = 0.71073)	Mo Kα (λ = 0.71073)	MoKα (λ = 0.71073)
2θ range for data collection/°	4.63 to 57.14	3.26 to 46.5	4.366 to 57.208
Index ranges	-23 ≤ h ≤ 23, -13 ≤ k ≤ 13, -21 ≤ l ≤ 22	-22 ≤ h ≤ 22, -11 ≤ k ≤ 11, -27 ≤ l ≤ 27	-15 ≤ h ≤ 15, -10 ≤ k ≤ 10, -20 ≤ l ≤ 21
Reflections collected	13853	19049	16509
Independent reflections	6617 [R _{int} = 0.0737, R _{sigma} = 0.1152]	3735 [R _{int} = 0.0510, R _{sigma} = 0.0411]	3736 [R _{int} = 0.0207, R _{sigma} = 0.0206]
Data/restraints/parameters	6617/8/330	3735/0/350	3736/1/270
Goodness-of-fit on F ²	1.002	1.073	1.030
Final R indexes [all data]	R ₁ = 0.0924, wR ₂ = 0.1710	R ₁ = 0.0604, wR ₂ = 0.1128	R ₁ = 0.0265, wR ₂ = 0.0704
Largest diff. peak/hole / e Å ⁻³	0.65/-0.87	0.61/-0.58	0.31/-0.16

$R_1 = \sum ||F_o| - |F_c|| / \sum |F_o|$. $wR_2 = [\sum w(|F_o| - |F_c|)^2 / \sum w(F_o)^2]^{1/2}$. $w = 0.75 / (\sigma^2(F_o) + 0.00010F_o^2)$.
 Goodness-of-fit = $\{\sum [w(F_o^2 - F_c^2)^2] / (n-p)\}^{1/2}$, where n is the number of reflections and p is the total number of parameters refined.

Single Crystal X-ray study of [Tp*TiCl₂pz*]pz* (2). In compound **2**, the titanium center is coordinated to two chloride ligands and 3 pyrazolyl moieties and one neutral pyrazole ligand, which has been scavenged from a sacrificial titanium species, **Figure 2**  an uncoordinated

pyrazole participates in hydrogen bonding. The free pyrazole molecule resides on a two-fold rotation axis in the $C2/c$ space group and was modelled for disorder. The average Ti-Cl bond length is 2.3727(12) Å and the average Ti-N bond length is 2.173(3) Å. The Ti-N_{pz} bond length is 2.186(3) Å. The average N-Ti-Cl total length is 4.544(3) Å, while the N-Ti-N_{pz} total length is slightly shorter at 4.345(4) Å. The Cl-Ti-Cl bond angle is 95.41 Å and the average N-Ti-N angle is 85.71(10)°. The average Cl-Ti-N_{pz} bond angle is 90.32(8)°.

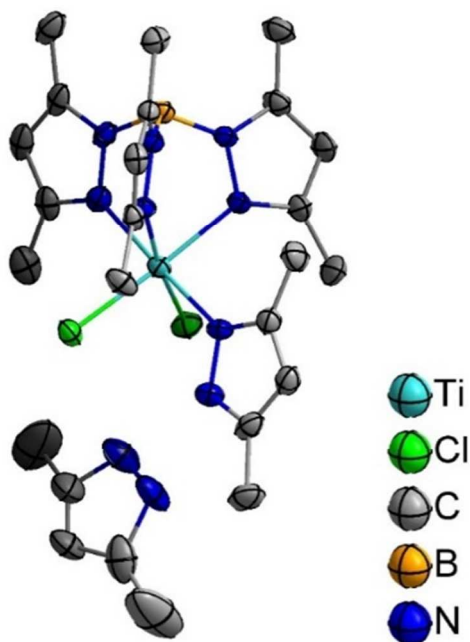


Figure S1 (a) Depiction of the asymmetric unit of [Tp*TiCl₂pz*][pz*], **2**, with thermal ellipsoids plotted at the 50% probability level; H atoms are omitted for the sake of clarity. Coordinated and uncoordinated pyrazole ligands are depicted which are evidence of Ti^{III} reactivity in cleaving the Tp* ligand.

Table S2. Bond Distances for compound **1**.

Atom	Atom	Length/Å	Atom	Atom	Length/Å
Ti1	Cl1	2.3954(18)	C23	C22	1.502(8)
Ti1	N1	2.194(5)	N5	N6	1.374(6)

Ti1	C12	2.3923(16)	N5	C12	1.340(7)
Ti1	N3	2.193(5)	C14	N6	1.364(7)
Ti1	C13	2.3811(17)	C14	C13	1.377(9)
Ti1	N5	2.213(5)	C14	C15	1.502(8)
N1	N2	1.375(6)	C6	C7	1.508(7)
N1	C2	1.349(7)	C7	C8	1.383(8)
C1	C2	1.483(7)	N7	C22	1.532(7)
B1	N2	1.546(7)	N7	C18	1.513(8)
B1	N4	1.547(7)	N7	C16	1.526(7)
B1	N6	1.515(8)	N7	C20	1.513(7)
N2	C4	1.364(7)	C10	C9	1.503(7)
C2	C3	1.401(8)	C8	C9	1.378(8)
N3	N4	1.384(6)	C13	C12	1.413(8)
N3	C7	1.347(7)	C12	C11	1.495(9)
C3	C4	1.380(7)	C19	C18	1.508(9)
N4	C9	1.359(7)	C17	C16	1.518(9)
C4	C5	1.490(7)	C20	C21	1.491(9)

Table S3. Bond Distances for compound **1**.

Atom	Atom	Atom	Angle/°	Atom	Atom	Atom	Angle/°
N1	Ti1	C11	89.55(13)	C3	C4	N2	106.8(4)
C12	Ti1	C11	96.79(6)	C5	C4	N2	123.7(5)

C12	Ti1	N1	89.39(13)	C5	C4	C3	129.5(5)
N3	Ti1	Cl1	171.92(12)	N6	N5	Ti1	117.8(3)
N3	Ti1	N1	85.41(17)	C12	N5	Ti1	134.1(4)
N3	Ti1	Cl2	89.47(12)	C12	N5	N6	107.8(4)
Cl3	Ti1	Cl1	94.08(6)	C13	C14	N6	108.4(5)
Cl3	Ti1	N1	174.42(12)	C15	C14	N6	122.0(5)
Cl3	Ti1	Cl2	94.38(6)	C15	C14	C13	129.6(5)
Cl3	Ti1	N3	90.51(12)	N5	N6	B1	120.6(4)
N5	Ti1	Cl1	91.13(12)	C14	N6	B1	130.5(5)
N5	Ti1	N1	85.43(17)	C14	N6	N5	108.9(5)
N5	Ti1	Cl2	170.50(13)	C6	C7	N3	122.8(5)
N5	Ti1	N3	82.20(16)	C8	C7	N3	110.5(4)
N5	Ti1	Cl3	90.26(12)	C8	C7	C6	126.7(5)
N2	N1	Ti1	118.7(3)	C18	N7	C22	110.9(4)
C2	N1	Ti1	134.7(4)	C16	N7	C22	108.3(4)
C2	N1	N2	106.6(4)	C16	N7	C18	108.6(4)
N4	B1	N2	109.6(4)	C20	N7	C22	108.4(4)
N6	B1	N2	109.7(5)	C20	N7	C18	109.9(4)
N6	B1	N4	109.8(4)	C20	N7	C16	110.8(4)
B1	N2	N1	119.8(4)	C9	C8	C7	106.4(5)
C4	N2	N1	110.4(4)	C12	C13	C14	105.9(5)
C4	N2	B1	129.7(4)	C13	C12	N5	109.0(5)
C1	C2	N1	123.8(5)	C11	C12	N5	124.9(5)
C3	C2	N1	109.3(5)	C11	C12	C13	126.0(5)
C3	C2	C1	126.9(5)	C10	C9	N4	124.0(5)
N4	N3	Ti1	118.8(3)	C8	C9	N4	107.4(5)
C7	N3	Ti1	135.6(3)	C8	C9	C10	128.5(5)
C7	N3	N4	105.6(4)	N7	C22	C23	114.2(5)
C4	C3	C2	106.9(5)	C19	C18	N7	116.0(5)
N3	N4	B1	119.3(4)	C17	C16	N7	115.0(5)
C9	N4	B1	130.6(4)	C21	C20	N7	115.6(5)
C9	N4	N3	109.9(4)				

Table S4. Bond Distances for compound **2**.

Atom	Atom	Length/Å	Atom	Atom	Length/Å
Ti1	Cl1	2.3868(12)	N6	C14	1.353(4)
Ti1	N1	2.165(3)	C7	C8	1.388(5)
Ti1	Cl2	2.3585(11)	N7	C17	1.342(4)

Ti1	N3	2.183(2)	N7	N8	1.367(4)
Ti1	N5	2.171(3)	C11	C12	1.498(4)
Ti1	N8	2.186(3)	C10	C9	1.492(5)
C1	C2	1.489(5)	C9	C8	1.373(5)
B1	N2	1.532(5)	C12	C13	1.389(5)
B1	N4	1.542(5)	C13	C14	1.378(4)
B1	N6	1.538(5)	C16	C17	1.500(5)
N1	N2	1.378(4)	C15	C14	1.492(5)
N1	C2	1.348(4)	C17	C18	1.363(5)
N2	C4	1.352(4)	C20	C19	1.483(5)
C2	C3	1.390(5)	C21	C22	1.455(7)
C3	C4	1.374(5)	C22	C1a ¹	1.237(9)
N3	N4	1.384(3)	C22	C1a	1.428(9)
N3	C7	1.344(4)	C22	N9	1.506(8)
N5	N6	1.384(3)	C22	N10 ¹	1.330(7)
N5	C12	1.350(4)	C19	C18	1.393(5)
C5	C4	1.495(5)	C19	N8	1.353(4)
N4	C9	1.351(4)	N9	N10	1.353(9)
C6	C7	1.497(5)			

¹-X,+Y,1/2-Z

Table S5. Bond Angles for compound **2**.

Atom	Atom	Atom	Angle/°	Atom	Atom	Atom	Angle/°
N1	Ti1	C11	93.88(8)	N5	N6	B1	120.3(3)
Cl2	Ti1	C11	95.41(4)	C14	N6	B1	130.1(3)
Cl2	Ti1	N1	92.41(7)	C14	N6	N5	109.5(2)

N3	Ti1	C11	87.87(8)	C6	C7	N3	123.0(3)
N3	Ti1	N1	85.98(9)	C8	C7	N3	109.6(3)
N3	Ti1	C12	176.44(8)	C8	C7	C6	127.4(3)
N5	Ti1	C11	173.01(7)	N8	N7	C17	112.2(3)
N5	Ti1	N1	86.01(10)	C10	C9	N4	123.4(3)
N5	Ti1	C12	91.57(7)	C8	C9	N4	107.6(3)
N5	Ti1	N3	85.15(10)	C8	C9	C10	129.0(3)
N8	Ti1	C11	91.94(8)	C11	C12	N5	122.9(3)
N8	Ti1	N1	173.94(11)	C13	C12	N5	109.7(3)
N8	Ti1	C12	88.69(7)	C13	C12	C11	127.3(3)
N8	Ti1	N3	92.58(9)	C14	C13	C12	106.4(3)
N8	Ti1	N5	88.01(10)	C13	C14	N6	108.0(3)
N4	B1	N2	109.8(3)	C15	C14	N6	122.6(3)
N6	B1	N2	109.4(3)	C15	C14	C13	129.4(3)
N6	B1	N4	108.5(3)	C16	C17	N7	121.4(3)
N2	N1	Ti1	117.58(18)	C18	C17	N7	106.6(3)
C2	N1	Ti1	135.1(2)	C18	C17	C16	132.0(3)
C2	N1	N2	106.6(3)	C1a ¹	C22	C21	140.7(6)
N1	N2	B1	120.0(2)	C1a	C22	C21	141.1(6)
C4	N2	B1	130.0(3)	N9	C22	C21	118.9(4)
C4	N2	N1	110.0(3)	N9	C22	C1a ¹	54.8(5)
N1	C2	C1	122.3(3)	N9	C22	C1a	99.8(5)
C3	C2	C1	128.7(3)	N10 ¹	C22	C21	101.9(5)
C3	C2	N1	108.9(3)	N10 ¹	C22	C1a	60.5(5)
C4	C3	C2	107.2(3)	N10 ¹	C22	C1a ¹	115.2(6)
N4	N3	Ti1	116.72(17)	N10 ¹	C22	N9	117.0(5)
C7	N3	Ti1	136.5(2)	C18	C19	C20	126.9(3)
C7	N3	N4	106.3(2)	N8	C19	C20	123.2(3)
N6	N5	Ti1	116.96(19)	N8	C19	C18	109.9(3)
C12	N5	Ti1	136.3(2)	C19	C18	C17	106.9(3)
C12	N5	N6	106.3(3)	C9	C8	C7	106.8(3)
N3	N4	B1	120.2(2)	N7	N8	Ti1	119.2(2)
C9	N4	B1	130.1(3)	C19	N8	Ti1	136.3(2)
C9	N4	N3	109.6(2)	C19	N8	N7	104.5(3)
C3	C4	N2	107.2(3)	N10	N9	C22	107.6(5)
C5	C4	N2	123.4(3)	N9	N10	C22 ¹	105.5(6)
C5	C4	C3	129.4(3)				

$$^1-X,+Y,1/2-Z$$

Table S6. Bond Distances for compound **3**.

Atom	Atom	Length/Å	Atom	Atom	Length/Å
Ti1	C1	2.178(3)	N5	N6	1.3759(19)
Ti1	C2 ¹	2.1741(19)	N5	C9	1.346(2)
Ti1	C2	2.1741(19)	C5	C6	1.374(4)
Ti1	N3	2.137(2)	N6	C11	1.343(2)
Ti1	N5	2.1619(14)	C6	C7	1.497(4)
Ti1	N5 ¹	2.1619(14)	N7	C13	1.519(3)
N1	C1	1.166(4)	N7	C15	1.517(3)
B1	N4	1.545(3)	N7	C17 ¹	1.515(2)
B1	N6 ¹	1.547(2)	N7	C17	1.515(2)
B1	N6	1.547(2)	C8	C9	1.481(3)
N2	C2	1.161(3)	C9	C10	1.390(3)
N3	N4	1.380(3)	C10	C11	1.383(3)
N3	C4	1.346(3)	C11	C12	1.490(2)
C3	C4	1.493(4)	C13	C14	1.513(4)
N4	C6	1.345(3)	C15	C16	1.502(4)
C4	C5	1.385(4)	C17	C18	1.506(3)

$$^1-X,+Y,+Z$$

Table S7. Bond Angles for compound **3**.

Atom	Atom	Atom	Angle/°	Atom	Atom	Atom	Angle/°
C2	Ti1	C1	89.71(7)	C5	C4	C3	127.6(2)
C2 ¹	Ti1	C1	89.71(7)	N6	N5	Ti1	117.84(10)
C2 ¹	Ti1	C2	98.36(10)	C9	N5	Ti1	135.91(13)
N3	Ti1	C1	179.95(9)	C9	N5	N6	106.24(14)
N3	Ti1	C2	90.25(6)	C6	C5	C4	106.4(2)
N3	Ti1	C2 ¹	90.25(6)	N5	N6	B1	120.34(14)
N3	Ti1	N5	86.56(6)	C11	N6	B1	129.33(16)
N3	Ti1	N5 ¹	86.56(6)	C11	N6	N5	110.32(14)
N5 ¹	Ti1	C1	93.47(6)	N4	C6	C5	108.0(2)
N5	Ti1	C1	93.48(6)	N4	C6	C7	122.4(3)
N5	Ti1	C2 ¹	172.39(6)	C5	C6	C7	129.6(3)

N5 ¹	Ti1	C2 ¹	88.57(6)	C15	N7	C13	105.6(2)
N5 ¹	Ti1	C2	172.39(6)	C17	N7	C13	111.83(13)
N5	Ti1	C2	88.57(6)	C17 ¹	N7	C13	111.83(13)
N5 ¹	Ti1	N5	84.34(8)	C17 ¹	N7	C15	110.99(13)
N1	C1	Ti1	174.0(2)	C17	N7	C15	110.99(13)
N4	B1	N6	109.42(13)	C17 ¹	N7	C17	105.71(18)
N4	B1	N6 ¹	109.42(13)	N5	C9	C8	122.45(17)
N6 ¹	B1	N6	107.45(19)	N5	C9	C10	109.65(17)
N2	C2	Ti1	173.43(17)	C10	C9	C8	127.90(17)
N4	N3	Ti1	118.42(14)	C11	C10	C9	106.28(15)
C4	N3	Ti1	135.34(17)	N6	C11	C10	107.51(15)
C4	N3	N4	106.2(2)	N6	C11	C12	124.10(17)
N3	N4	B1	120.16(18)	C10	C11	C12	128.39(17)
C6	N4	B1	130.2(2)	C14	C13	N7	114.7(2)
C6	N4	N3	109.7(2)	C16	C15	N7	115.6(2)
N3	C4	C3	122.7(2)	C18	C17	N7	114.88(17)
N3	C4	C5	109.7(2)				

¹-X,+Y,+Z

Magnetism

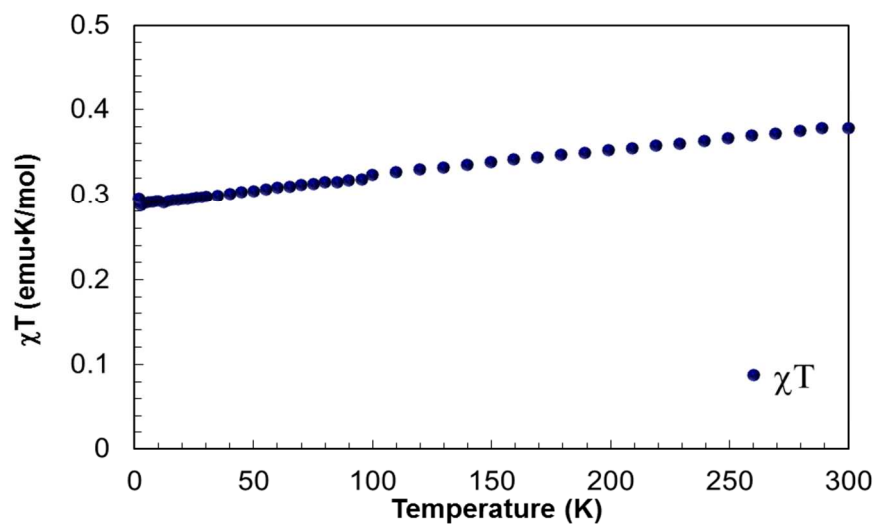


Figure S2. Temperature dependence of χT for **1**. The linear decrease in the χT product is due to van Vleck temperature independent paramagnetism (TIP).

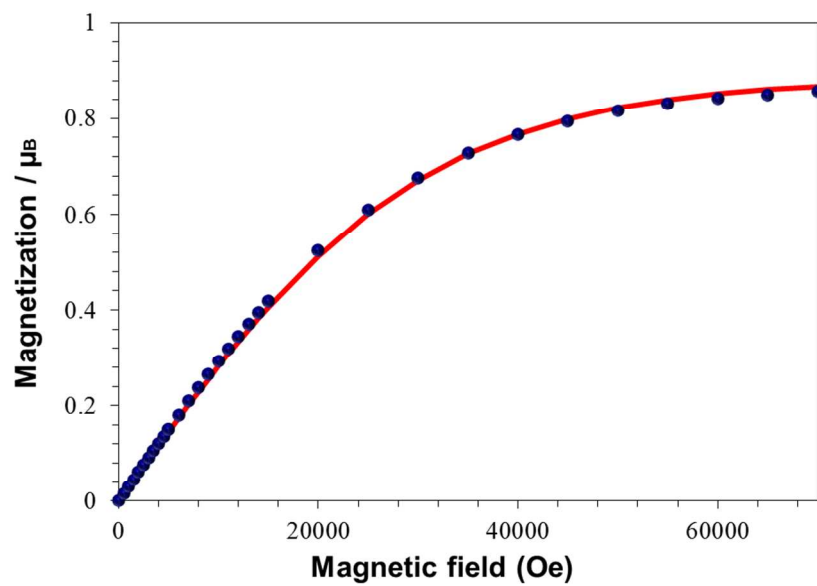


Figure S3. Best fit of the magnetization (blue data points) data for **1** to the Brillouin function (red line) at 1.8 K. The best fit leads to a g value of ~ 1.77 at this temperature.

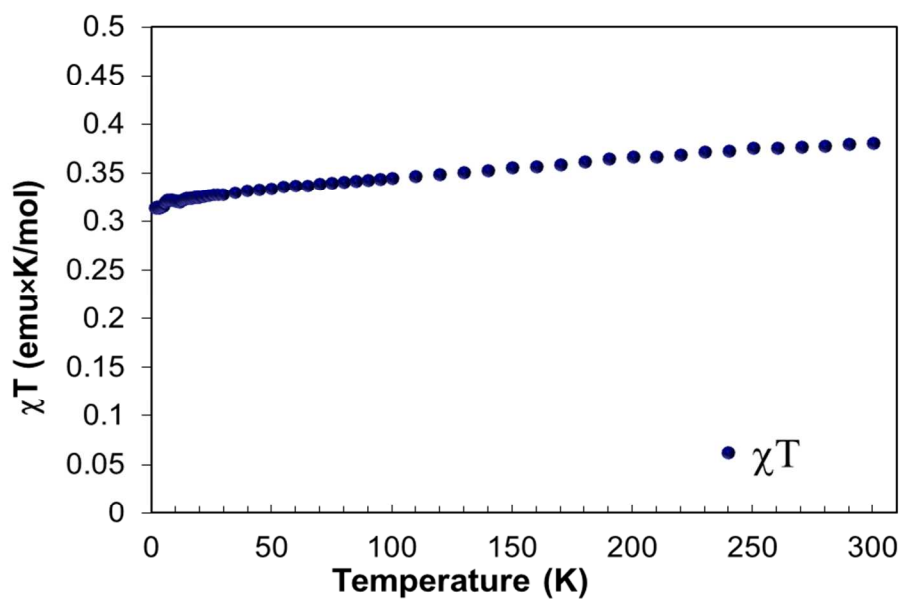


Figure S4. Temperature dependence of χT for **3**. The linear decrease in the χT product is due to van Vleck temperature independent paramagnetism (TIP).

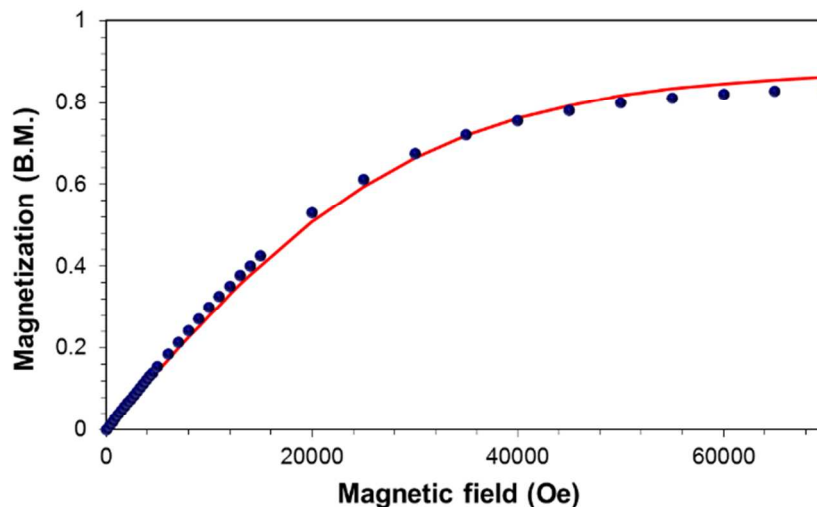


Figure S5. Magnetization vs magnetic field plot for **3**. The red line represents the best fit to the Brillouin function.

Computational Details

Ab initio calculations were performed on the crystallographic structure of the anions of compounds **1** and **3**, using the MOLCAS 7.6 software.⁷ We used basis sets from the MOLCAS 7.6 library: the ANO–RCC basis set on Ti, contracted to [6s5p3d2f], in combination with ANO–S basis sets on all other atoms, contracted to [4s3p1d] on Cl, [3s2p1d] on B, N, and the cyanide carbon atoms, [3s2p] on the remaining carbon atoms, and [2s] on H.

After some trial calculations, an active space of 11 electrons in 10 orbitals was selected for both compounds. It consists of the Ti 3p shell, the 3d shell, and a bonding e_g pair of orbitals which show substantial covalency between ligand and metal d orbitals. The ligand field states were obtained from a state-averaged CASSCF calculation over five roots. The Ti 3s orbital was kept frozen in the CASSCF calculation to prevent it from entering in the active space. In the subsequent CASPT2 step all but the core electrons (these are 1s of B, C and N; 1s, 2s, 2p and 3s of Ti) were correlated. An imaginary level shift of 0.1 Hartree was applied.

Spin–orbit coupling was introduced by diagonalization of an approximate atomic mean-field spin–orbit operator in the basis of the CASSCF wave functions with corresponding CASPT2 diagonal energies, using the RASSI module in MOLCAS. Subsequent magnetic susceptibility and g-factor calculations were done with the SINGLE_ANISO module in MOLCAS.

REFERENCES

- (1) Carlin, R. L. *Magnetochemistry*; Springer-Verlag: Berlin, 1986.
- (2) SMART and SAINT, Siemens Analytical X-Ray Instruments, I. Madison, WI, USA 1996
- (3) Sheldrick, G. M. *SADABS. Program for Empirical Absorption Correction.*; University of Gottingen: Germany, 1996.
- (4) Sheldrick, G. M. *Acta Crystallogr., Sect. A.* **2008**, *64*, 112.
- (5) Barbour, L. J. *J. Supramol. Chem.* **2001**, *1*, 189.
- (6) Pennington, W. J. *Appl. Crystallogr.* **1999**, *32*, 1028.

(7) F. Aquilante, L. De Vico, N. Ferré, G. Ghigo, P.-Å Malmqvist, P. Neogrády, T.B. Pedersen, M. Pitonak, M. Reiher, B.O. Roos, L. Serrano-Andrés, M. Urban, V. Veryazov, R. Lindh, MOLCAS 7: the next generation, *J. Comput. Chem.*, 2010, **31**, 224-247.